Electrical and optical properties of boron-doped ZnO thin films for solar cells grown by metalorganic chemical vapor deposition

Wilson W. Wenas, Akira Yamada, and Kiyoshi Takahashi
Department of Physical Electronics, Tokyo Institute of Technology, 2-12-1, Ohokayama, Meguro-ku, Tokyo 152, Japan

Masahiro Yoshino and Makoto Konagai
Department of Electrical and Electronic Engineering, Tokyo Institute of Technology, 2-12-1, Ohokayama, Meguro-ku, Tokyo 152, Japan

(Received 20 May 1991; accepted for publication 3 September 1991)

The highly conductive and textured ZnO films have been grown by metalorganic chemical vapor deposition using diethylzinc and H_2O as reactant gases. The B_2H_6 gas has also been successfully used as an *n*-type dopant gas to obtain highly conductive ZnO with a sheet resistivity for 2-μm-thick film as low as 10 $\Omega/\square$ at the very low temperature of 150 °C. It was found that the crystal orientation and grain structure change with B_2H_6 flow rate. The decreasing of the film transmittance due to the free-carrier absorption in the wavelength region above 1000 nm was observed and it seems that the impurity scattering was the dominant interaction during this process. The shift of the absorption edge due to band filling was also observed as the B_2H_6 flow rate was increased.

I. INTRODUCTION

ZnO thin film has been applied to many devices such as surface-acoustic-wave devices,[1] solar cells,[2] and other optoelectronic devices. Unfortunately, the different applications of ZnO thin films to the various devices require different physical properties of films, which means a difference of deposition conditions. For solar cell applications, especially with transparent conducting oxide (TCO), the development of low resistive ZnO thin films along with textured high transparency is important.[3,4] ZnO has been attractive for solar cell applications, especially with *a*-Si (Ref. 5) and $CuInSe_2$ (Ref. 6) solar cells, because of its low cost and because it can be grown at relatively low temperature, compared to SnO_2 or indium tin oxide (ITO). Furthermore, it has been recognized that the conversion efficiency of solar cells can be improved by using textured ZnO films as a tranparent front electrode and an antireflection coating.[6] Therefore, it is strongly required to grow textured ZnO films for solar cell application. Several deposition techniques for obtaining ZnO thin films have been reported, such as sputtering,[7–11] spray pyrolysis,[12] and metalorganic chemical vapor deposition.[13–20] However, there are almost no papers describing the preparation of the textured ZnO films.

ZnO has an *n*-type wide band gap with a wurtzite crystal structure. The nonstochiometric undoped ZnO thin films usually show a low resistivity due to the oxygen vacancies and zinc interstitials. Hence, the low-resistivity film can be obtained by controlling these native defects. Nevertheless, many attempts have been made to obtain the low-resistivity ZnO films by doping with group-III elements such as aluminum,[21] indium,[22] or group-VII elements such as fluorine,[23] because it has been remarked that the extrinsic donors due to the dopant atoms are more stable than the intrinsic donors due to the native defects. In this study boron doping using B_2H_6 diluted with H_2 as a dopant gas was carried out to obtain the low-resistivity films.

II. EXPERIMENT

In this experiment, diethylzinc (DEZ) and H_2O were contained in bubblers and were kept in temperature-controlled baths. These reactant gases were bubbled with purified Ar gas. The flow rates of DEZ and H_2O transported to the growth chamber were set to 10.4 and 26.8 μmol/min, respectively. The flow rate of B_2H_6 transported to the chamber was varied from 0.05 to 0.7 μmol/min. ZnO films were grown on Corning 7059 glass substrate and the substrate temperature was varied from 100 to 300 °C. The total pressure was kept at 6 Torr. The crystal orientation and the surface morphology of the films were evaluated by x-ray diffraction and scanning electron microscopy (SEM), respectively. The Hall measurement using a van der Pauw configuration was used to evaluate the electrical properties of the obtained films.

III. RESULTS AND DISCUSSION

In the previous work, we have reported the preparation of textured ZnO.[24] It has been remarked that the surface morphology of the film is strongly dependent on the substrate temperature. At the relatively low substrate temperature of 150 °C, the film surface shows a tetrapodlike morphology with a macroscopic haze.

In this study, *n*-type doping using B_2H_6 diluted with H_2 has been attempted to obtain highly conductive ZnO. The electrical properties of B_2H_6-doped ZnO films as a function of substrate temperature are shown in Fig. 1. It is clear that the electrical properties of these films are strongly dependent on substrate temperature. Up to 150 °C, the mobility increases with the substrate temperature but above 150 °C it decreases. The carrier concentration also indicates the same pattern as mobility. Below 150 °C, carrier concentration increases with substrate temperature but becomes constant and tends to decrease at higher temperatures. The change of mobility and carrier concentration with substrate temperature is most probably

 0021-8979/91/117119-05$03.00

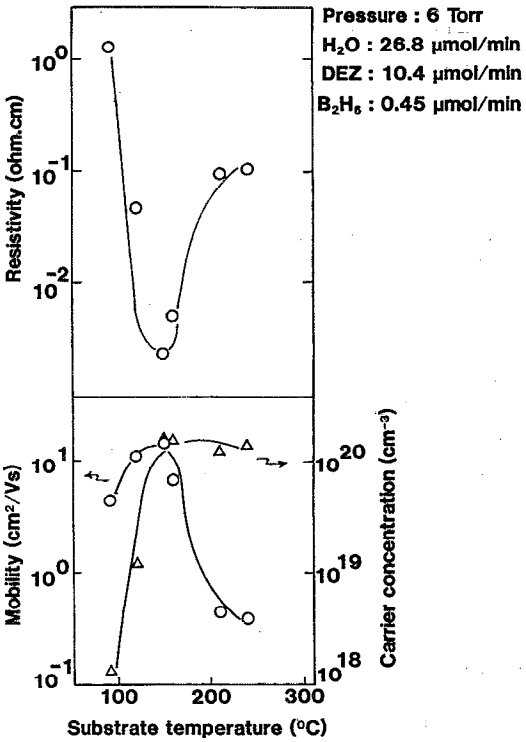

FIG. 1. Electrical properties of boron-doped ZnO as a function of substrate temperature.

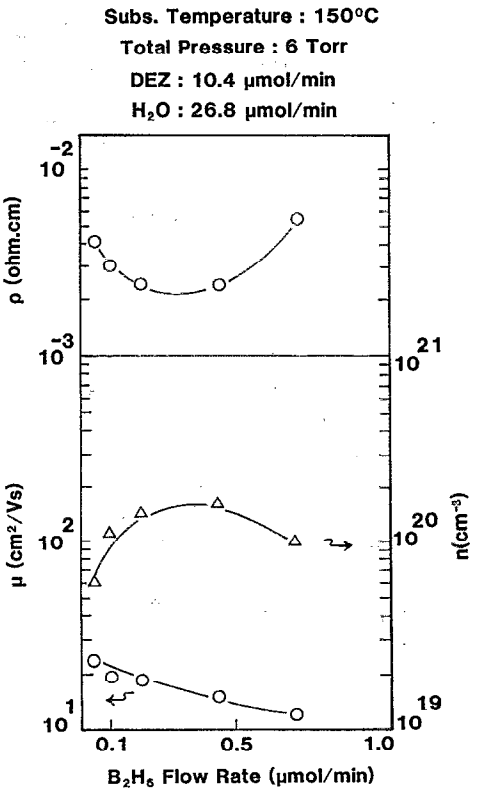

FIG. 3. Dependence of the electrical properties of ZnO films on B_2H_6 flow rate.

due to the changing of the crystal orientation or grain structure. The crystal orientation and grain size of the obtained films were evaluated by the SEM and x-ray diffraction measurements.

SEM photographs of films are shown in Fig. 2. At the substrate temperature of 90 °C, the surface morphology of the film shows granular crystallites with a mirrorlike morphology. This film has a (002) reflection peak with a strong intensity, suggesting that the grains have a *c* axis perpendicular to the substrate surface.[24] At 150 °C the film shows a textured morphology with a macroscopic haze, which indicates that most grains have a *c* axis parallel to the substrate surface and the (100) and (110) reflection peaks are dominant. However, at 240 °C the textured morphology becomes disordered and the (100) and (110) reflection peaks become less pronounced. The changing of the surface morphology with substrate temperature is probably due to the difference of the surface energy of the ZnO crystallite structure. The net effect of the substrate temperature dependence of the films is that the resistivity reaches its lowest value at a substrate temperature of around 150 °C. It can be seen thus that at a substrate temperature of 150 °C, the obtained films have low resistivity in addition to textured morphology. This temperature is very low compared with the growth temperature of the other TCO materials. Therefore, it can be used for growing ZnO films for solar cell applications such as *a*-Si and $CuInSe_2$ solar cells without affecting the device's performance.

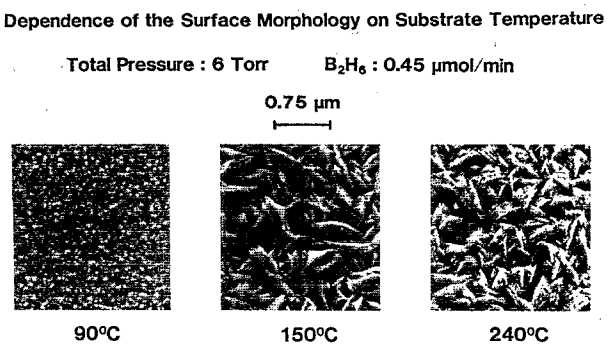

To improve the electrical properties of the obtained films for solar cell applications, the flow rate of B_2H_6 as a dopant gas has been varied from 0.05 to 0.7 μmol/min. Figure 3 shows the electrical properties of those obtained films. The mobility decreases gradually as the flow rate of B_2H_6 is increased. The electron concentration increases as the flow rate of B_2H_6 is increased up to 4.5 μmol/min and decreases at the higher B_2H_6 flow rate. The increase of the carrier concentration at the B_2H_6 flow rate of up to 4.5 μmol/min results from extrinsic donors due to boron substitution at the Zn site and/or the boron interstitial in the ZnO lattice.[21] However, the carrier concentration decreases at a B_2H_6 flow rate of 0.7 μmol/min. To clarify this point, the boron atom concentration in the film was measured by using secondary-ion mass spectrometry (SIMS),

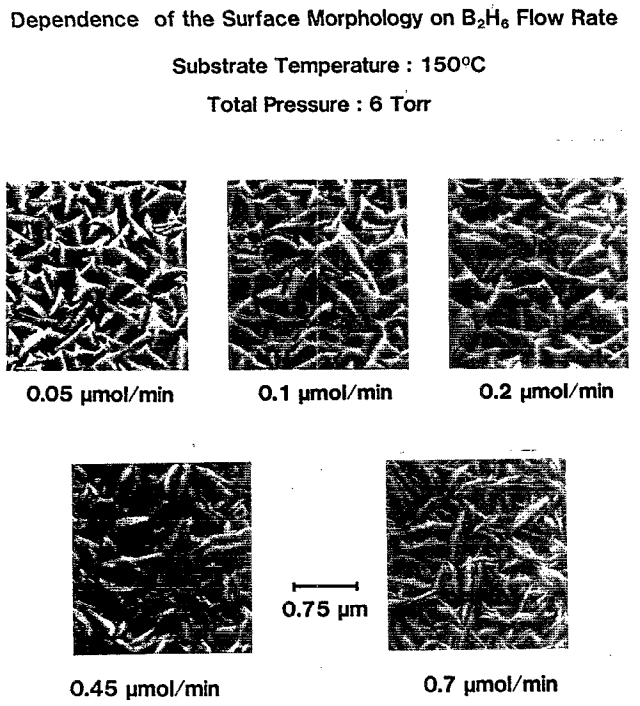

FIG. 4. SEM photographs of ZnO films deposited at various B_2H_6 flow rates.

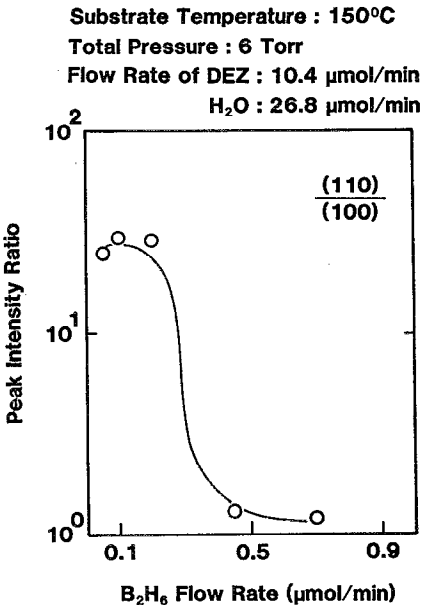

FIG. 5. Ratio of x-ray diffraction intensities of ZnO films [(110)/(100)] as a function of B_2H_6 flow rate.

and it is found that the boron atom concentration was around 2×10^{21} cm^{-3}. Since the measured carrier concentration is around 2×10^{20} cm^{-3}, only about 10% of the boron atoms in the film are electrically active. This result suggests the existence of the defects and the compensation mechanism. Therefore, the decrease of carrier concentration in the film at a B_2H_6 flow rate of 0.7 μmol/min can be explained by an increase in defect density and/or in activity of the compensation mechanism. Furthermore, the decrease of mobility with increased B_2H_6 flow rate indicates the role of impurity scattering, as will be confirmed later.

The scanning electron microscopy photographs of these films have been taken to evaluate their surface morphology and grain structure, and are shown in Fig. 4. The SEM photographs show that all of the obtained films have a textured morphology with a macroscopic haze, but that the surface morphology of the films changes with B_2H_6 flow rate. Up to 0.2 μmol/min, films show a tetrapodlike morphology and above 0.2 μmol/min the tetrapod shapes deteriorate. The crystal orientation of these films were also evaluated by x-ray diffraction. Only (100) and (110) reflection peaks appear in all of those films. This result indicates that the *c*-axis orientations are parallel to the substrate surface. Figure 5 shows the x-ray diffraction intensity ratio of those films [(110)/(100)] as a function of B_2H_6 flow rate. The (110) reflection peak becomes less pronounced as the B_2H_6 flow rate is increased. These results agree well with those of the SEM photographs. Since the obtained films have various kinds of textured morphologies, further investigation is needed to choose the best candidate film to be a window layer for solar cells.

The transparency of the obtained films was characterized to confirm that it was appropriate for solar cell application. The transparency was assessed from the transmittance measured by the double-beam monochromator in atmospheric ambient at wavelengths from 300 to 1400 nm. As shown in Fig. 6, the transmittance decreases as B_2H_6 is increased at wavelengths above 1000 nm. This is because of the free-carrier absorption which increases as the carrier concentration increases. To confirm this statement, the absorption coefficient was calculated and a linear relationship was obtained by plotting the absorption coefficient versus the 3.5 power of the wavelength, as shown in Fig. 7. This result suggests that the ionized impurity scattering is the dominant scattering interaction with electrons before they reach their final state in the photon absorption process.[25] From this result, it can also be concluded that the decrease of film transmittance at the B_2H_6 flow rate of 0.7 μmol/min, where the carrier concentration was seen to decrease,

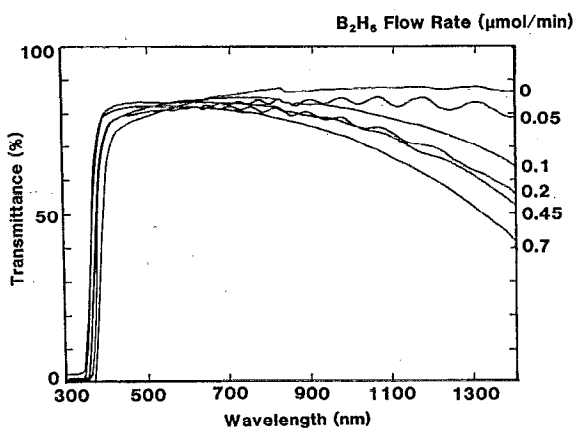

FIG. 6. Transmittance of the ZnO films at various B_2H_6 flow rates.

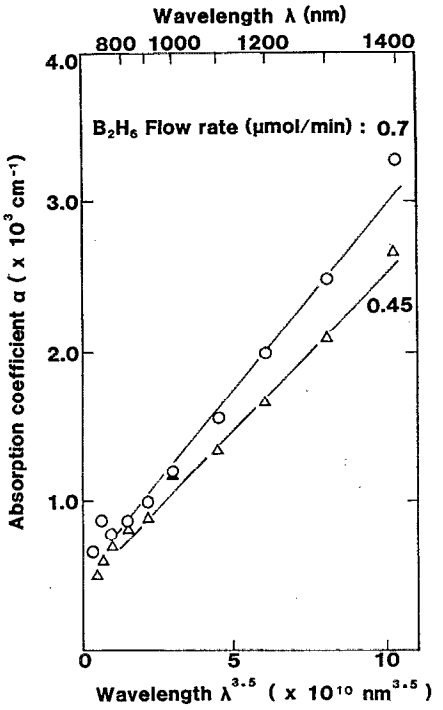

FIG. 7. Absorption coefficient of ZnO films as a function of the 3.5 power of wavelength.

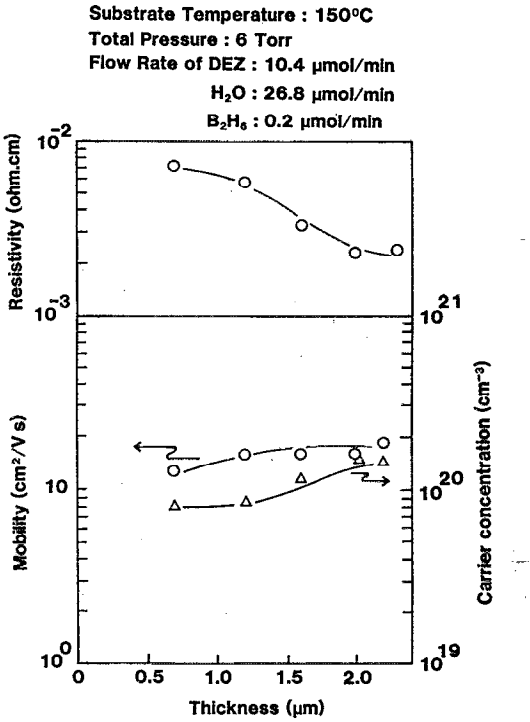

FIG. 8. Dependence of the electrical properties of ZnO film on its thickness.

is due to an increase in ionized impurity concentration, because the increase of impurity scattering will reduce the carrier relaxation time, which is inversely proportional to the carrier absorption. Thus, in our highly doped samples, the carrier concentration is not equal to the ionized impurity concentration. The above result indicates that the ionized impurity concentration of the 0.7-μmol/min B_2H_6-doped film is higher than that of the 0.45-μmol/min B_2H_6-doped film due to the higher defect density and/or due to the higher activity of the compensation mechanism.

It also can be seen from Fig. 6 that the optical gap increases as the B_2H_6 flow rate is increased. This effect is known as the Burstein–Moss shift,[26,27] where in the heavily doped *n*-type semiconductor, the Fermi level is inside the conduction band and the states near the bottom of the conduction band are filled. Therefore, the absorption edge should shift to higher energy.

The dependence of the electrical properties and surface morphology on the film thickness were also evaluated. Figure 8 shows the Hall measurement of the obtained film as a function of its thickness. Both mobility and carrier concentration increase with film thickness. The net effect is a decrease of the film resistivity. The decrease of the resistivity with film thickness may be attributed to the nonuniform growth of the film grain structure as the film thickens. SEM photographs of these films have been taken to affirm this and are shown in Fig. 9. The shape of the tetrapodlike morphology does not change with film thickness but the grain size becomes greater as the film thickness is increased. This result indicates that the grain is not uniform for all film thicknesses. This nonuniformity is probably due to the high growth rate of films.

The obtained ZnO films have been applied to the preliminary stage of $CuInSe_2$ solar cells as transparent front electrodes and antireflection coatings to obtain a short-circuit current density as high as 44.9 mA/cm^2. This result shows the important role which textured ZnO films can play in lengthening the optical path length of the incident light through the multiple reflections.

IV. CONCLUSION

In this study, textured and low-resistivity ZnO thin films have been obtained. The B_2H_6 gas has been successfully used as an *n*-type dopant to obtain low-resistivity films. It was also found that the electrical properties of films are strongly dependent on growth conditions. A sheet

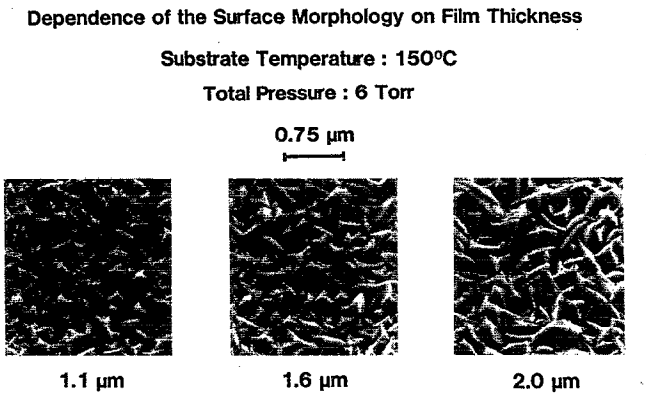

FIG. 9. SEM photographs of ZnO films at various film thicknesses.

resistivity for 2-μm-thick film as low as 10 $\Omega/\square$ was obtained at a very low substrate temperature of 150 °C. This result suggests that the obtained films are surely proper for solar cell applications. Furthermore, the crystal orientation and the grain structure changed with B_2H_6 flow rate. The decrease of the film transmittance due to the free-carrier absorption was observed in the wavelength region above 1000 nm, and it seems that the impurity scattering was the dominant interaction during this process. The Burstein–Moss shift effect due to band filling was also observed as the B_2H_6 flow rate was increased. The electrical properties of the film also changed with the film thickness. This may be caused by the nonuniformity of the grain structure growth as the film thickens. Further investigations are under way to improve the grain structure of ZnO films.

ACKNOWLEDGMENTS

This work was support in part by the Agency of Industrial Science and Technology under the Sunshine Project, and by a Grant-in-Aid for Scientific Research from the Ministry of Education, Science and Culture.

[1] T. Mitsuyu, S. Ono, and K. Wasa, J. Appl. Phys. **51**, 2646 (1980).
[2] R. R. Potter, Solar Cells **16**, 521 (1986).
[3] H. Schade and Z. E. Smith, J. Appl. Phys. **57**, 568 (1985).
[4] S. Mayor and K. L. Chopra, Sol. Energy Mater. **17**, 319 (1988).
[5] A. Banerjee and G. Guha, J. Appl. Phys. **69**, 1030 (1991).
[6] D. Pier and K. Mitchell, *Proceedings of the 9th European Photovoltaic Solar Energy Conference*, edited by W. Palz, G. T. Wrixon, and P. Helm (Kluwer Academic, Dordrecht, Netherlands, 1989), p. 488.
[7] W. Webb, D. W. Williams, and M. Buchanan, Appl. Phys. Lett. **39**, 640 (1981).
[8] T. Minami, H. Nanto, and S. Sakata, Appl. Phys. Lett. **41**, 958 (1982).
[9] T. Minami, H. Sato, H. Nanto, and S. Takata, Jpn. J. Appl. Phys. **24**, L781 (1985).
[10] Y. Igasaki and H. Saito, J. Appl. Phys. **69**, 2190 (1991).
[11] R. E. I. Schropp and A. Madan, J. Appl. Phys. **66**, 2027 (1989).
[12] J. Aranovich, A. Ortiz, and R. H. Bube, J. Vac. Sci. Technol. **16**, 994 (1979).
[13] C. K. Lau, S. K. Tiku, and K. M. Lakin, J. Electrochem. Soc. **127**, 1843 (1980).
[14] S. Oda, H. Tokunaga, N. Kitajima, J. Hanna, I. Shimizu, and H. Kokado, Jpn. J. Appl. Phys. **24**, 1607 (1985).
[15] P. Souletie, S. Bethke, B. W. Wessels, and H. Pan, J. Cryst. Growth **86**, 248 (1988).
[16] T. Shiosaki, T. Yamamoto, M. Yagi, and A. Kawabata, Appl. Phys. Lett. **39**, 399 (1981).
[17] A. P. Roth and D. F. Williams, J. Appl. Phys. **52**, 6685 (1981).
[18] S. K. Gandhi, R. J. Field, and J. R. Field, Appl. Phys. Lett. **37**, 449 (1980).
[19] P. J. Wright, R. J. M. Griffiths, and B. Cockayne, J. Cryst. Growth **66**, 26 (1984).
[20] M. Shimizu, T. Katayama, Y. Tanaka, T. Shiosaki, and A. Kawabata, J. Cryst. Growth **101**, 171 (1990).
[21] S. Takada, T. Minami, and H. Nanto, Thin Solid Films **135**, 183 (1986).
[22] S. Mayor, A. Banerjee, and K. L. Chopra, Thin Solid Films **108**, 333 (1983).
[23] R. G. Gordon, J. Hu, C. Guinta, and J. Musher, SERI Annual Report Photovoltaic Program Branch FY 1989, edited by K. A. Summers (Colorado, 1990), p. 29.
[24] W. W. Wenas, A. Yamada, M. Konagai, and K. Takahashi, Jpn. J. Appl. Phys. **30**, L441 (1991).
[25] S. Visvanathan, Phys. Rev. **120**, 375 (1960).
[26] E. Burstein, Phys. Rev. **93**, 632 (1954).
[27] T. S. Moss, Proc. Phys. Soc. (London) Sect. B **76**, 775 (1954).